Article details

Maaden K. van der, Schipper P., Jiskoot W., Bouwstra J.A. (2019), Chemical Modifications of Gold Surfaces with Basic Groups and a Fluorescent Nanoparticle Adhesion Assay To Determine Their Surface pKa, Langmuir 35(22): 7121-7128
Doi: 10.1021/acs.langmuir.9b00139

LANGMUIR Article
Cite This: Langmuir 2019, 35, 7121−7128
pubs.acs.org/Langmuir

Chemical Modifications of Gold Surfaces with Basic Groups and a Fluorescent Nanoparticle Adhesion Assay To Determine Their Surface pK_a

K. van der Maaden,[‡,*] P. Schipper,[‡] W. Jiskoot, and J. A. Bouwstra

Division of BioTherapeutics, Leiden Academic Centre for Drug Research (LACDR), Leiden University, 2300 RA Leiden, The Netherlands

ABSTRACT: For pharmaceutical, biological, and biomedical applications, the functionalization of gold surfaces with pH-sensitive groups has great potential. The aim of this work was to modify gold surfaces with pH-sensitive groups and to determine the pK_a of the modified gold surfaces using a fluorescent nanoparticle adhesion assay. To introduce pH-sensitive groups onto gold surfaces, we modified gold-coated silicon slides with four different bases: 4-mercaptopyridine (4-MP), 4-pyridylethylmercaptan (4-PEM), 4-aminothiophenol (4-ATP), and 2-mercaptoethylamine (2-MEA). To screen whether the modifications were successful, the binding of negatively charged fluorescently labeled nanoparticles to the positively charged surfaces was visualized by fluorescence microscopy and atomic force microscopy. Next, the pK_a of the modified surfaces was determined by quantifying the pH-dependent adhesion of the fluorescently labeled nanoparticles with fluorescence spectroscopy. Fluorescence microscopy showed that the gold surfaces were successfully modified with the four different basic molecules. Moreover, fluorescence spectroscopy revealed that fluorescently labeled negatively charged nanoparticles bound onto gold surfaces that were modified with one of the four bases in a pH-dependent manner. By quantifying the adsorption of negatively charged fluorescently labeled nanoparticles onto the functionalized gold surfaces and using the Henderson−Hasselbalch equation, the pK_a of these surfaces was determined to be 3.7 ± 0.1 (4-MP), 5.0 ± 0.1 (4-PEM), 5.4 ± 0.1 (4-ATP), and 7.4 ± 0.3 (2-MEA). We successfully functionalized gold surfaces with four different basic molecules, yielding modified surfaces with different pK_a values, as determined with a fluorescent nanoparticle adhesion assay.

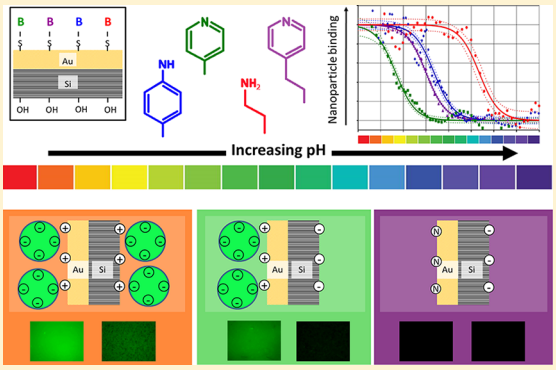

INTRODUCTION

Gold microstructures and nanoparticles are often researched for pharmaceutical, biological, and biomedical applications because of their biocompatible nature.[1] Microneedles, for example, which are needle-like structures with micrometer dimensions that are used for minimally invasive and pain-free dermal drug delivery or sampling of biological fluids[2] that are made of silicon, have been coated with a layer of gold.[3−5] Such gold-coated silicon microneedles have been functionalized to detect vancomycin.[3] Furthermore, gold nanoparticles are used for the delivery of genes[6] and anticancer drugs.[7,8] To further extend the applicability of gold microstructures and nanoparticles for pharmaceutical purposes, their surfaces can be functionalized with pH-sensitive groups. This will enable the immobilization/desorption of DNA, proteins, antigens, and nanoparticles via electrostatic interactions onto/from gold microstructures and nanoparticles as a function of the pH. Importantly, the success of pH-dependent drug delivery will depend on the pK_a of functionalized gold surfaces, which, in turn, depends on the choice of the functional group and has to be experimentally confirmed.

Fluorescent nanoparticles can be used to investigate the surface properties of chemically modified surfaces. Recently, we developed a fluorescent nanoparticle adhesion assay (FNAA) to determine the pK_a of silicon surfaces that are modified with acidic and basic molecules.[9] This method is based on pH-dependent adsorption of cationic or anionic fluorescent nanoparticles onto surfaces with an opposite charge via electrostatic interactions. So far, the FNAA has been used to determine the pK_a of silicon surfaces modified with amine groups (APTES),[9] carboxylic groups,[9] and pyridine groups.[10,11] Besides, this method was used to analyze more complex surfaces (i.e., determination and design of the isoelectric point of chemically modified silicon surfaces).[11] Furthermore, since most methods are not suitable to detect more than one pK_a values,[12] the FNAA could be an attractive method to analyze surfaces that have more than one pK_a values.[9] So far, the FNAA has not been used to determine the pK_a of surfaces other than silicon.

In this work, we modify gold-coated silicon surfaces with a panel of basic molecules. Such modified surfaces are potentially suitable for pharmaceutical applications. Besides, we used negatively charged fluorescently labeled nanoparticles and fluorescence

Received: January 14, 2019
Revised: March 28, 2019
Published: May 2, 2019

DOI: 10.1021/acs.langmuir.9b00139
Langmuir 2019, 35, 7121−7128

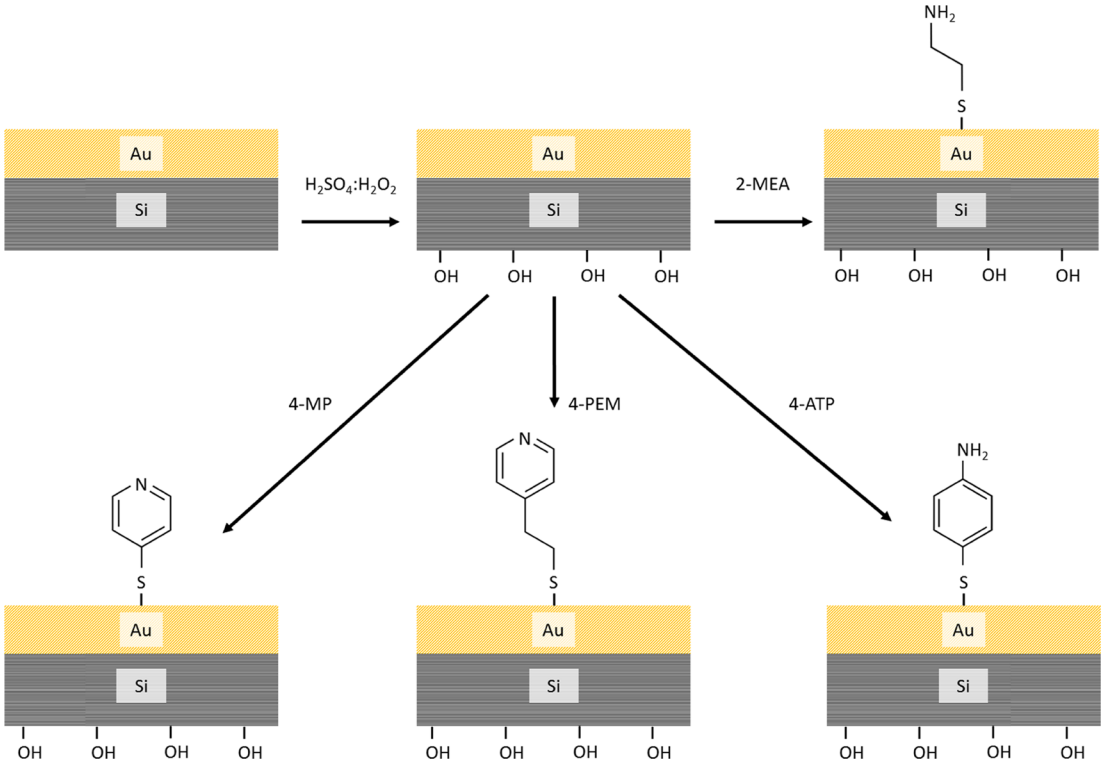

Figure 1. Introduction of pH-sensitive groups onto gold-coated silicon surfaces. Abbreviations: 2-MEA, 2-mercaptoethylamine; 4-MP, 4-mercaptopyridine; 4-PEM, 4-pyridylethylmercaptan; 4-ATP, 4-aminothiophenol.

microscopy to study the success of the modifications. Moreover, we show that, by determining the pH-dependent fluorescent nanoparticle adhesion onto gold-coated silicon slides, the pK_a of gold surfaces modified with a variety of basic molecules can be determined.

MATERIALS AND METHODS

Materials. Acetone (puriss), methanol (HPLC grade), hydrogen peroxide (30%, w/w; puriss p.a.), hydrochloric acid (HCl, 37%, ACS reagent grade), 4-mercaptopyridine (4-MP), 4-pyridylethylmercaptan (4-PEM), 4-aminothiophenol (4-ATP), 2-mercaptoethylamine (2-MEA), ethylenediaminetetraacetic acid (EDTA, ACS reagent grade), and 100 nm fluorescent orange sulfate-modified polystyrene latex beads (2.5% solids) were purchased from Sigma-Aldrich, Zwijndrecht, the Netherlands. Absolute ethanol (dehydrated, HPLC grade) was purchased from Biosolve, Valkenswaard, the Netherlands. Concentrated sulfuric acid (95−98%, ACS reagent grade) and sodium hydroxide (NaOH, ACS reagent grade) were ordered from Boom, Meppel, the Netherlands. Ultrapure deionized Milli-Q (MQ) water with a resistivity of 18 MΩ·cm was produced by an ELGA Purelab Ultra water purification system. BrandTech Scientific 1.5 mL cuvettes were purchased at VWR, Ede, the Netherlands. Black flat-bottom polystyrene 96-wells plates were obtained from Greiner Bio-One, Alphen a/d Rijn, the Netherlands.

Methods. *Preparation of Silicon Slides and Gold-Coated Silicon Slides.* Silicon wafers with <100> orientation and a thickness of 500 μm, one side of which was coated with a 1000 Å gold layer (Sigma-Aldrich), were diced into slides of 1 × 1 cm by using a General Signal Micro Automation Model 602 M dicing saw in conjunction with Disco ZH05 series dicing saws (further referred to as gold-coated silicon slides, having a gold-coated surface area of 1 cm^2 on one side and a noncoated (plain) silicon surface area of 1 cm^2 on the other side). To study nonspecific nanoparticle binding onto the (noncoated) silicon side of the gold-coated silicon slides, plain two-sided polished silicon wafers with <100> orientation and a thickness of 300 μm, which were cut into slides of 1 × 1 cm (further referred to as silicon control slides, having a total silicon surface area of 2 cm^2, obtained from Tyndall National Institute, Cork, Ireland), were used as a control.

Surface Modification. To obtain chemically modified gold surfaces with pH-sensitive groups, gold-coated silicon slides were modified with four different gold-reactive molecules, from which it was expected that they result in different surface pK_a values, as schematically represented in Figure 1. To simultaneously modify up to 45 silicon slides, polychlorotrifluoroethylene coating containers were developed by the fine mechanical department of Leiden University. Prior to the introduction of pH-sensitive surface groups, the slides were cleaned with acetone and methanol and were subsequently dried in a vacuum oven at 50 °C for 30 min. To remove residual organic contaminants, the slides were incubated in a piranha solution (7:3 (v/v) mixture of sulfuric acid and hydrogen peroxide) for 60 min at 120 °C (caution: piranha solution is an extremely corrosive mixture that should be treated with utmost carefulness). After removal of the piranha solution, the slides were washed with MQ water until the pH was above 5. Next, the slides were sequentially washed with methanol and dried.

To obtain pH-sensitive groups onto the gold-coated silicon slides, the slides were incubated overnight in a 10 mM solution of a gold-specific reactant (4-MP, 4-PEM, 4-ATP, or 2-MEA) in absolute ethanol at room temperature while gently rocking. Finally, nonreacted chemicals were removed by extensively washing the slides sequentially with absolute ethanol and methanol, after which the slides were dried. Slides were stored under vacuum until use. Silicon control slides, which were used to correct for nonspecific binding onto the silicon side of the gold-coated slides, were treated with the same procedure as gold-coated silicon slides.

Colloidal Stability of Nanoparticles as Function of pH. The pH-dependent colloidal stability of the 100 nm fluorescently labeled sulfate-modified negatively charged nanoparticles was assessed to investigate whether these nanoparticles are suitable to be used to determine the surface pK_a of the gold-coated silicon slides in the selected pH range (2−10). To this end, the pH-dependent hydrodynamic diameter and polydispersity index (PDI) of these nanoparticles were determined by using dynamic light scattering and the ζ-potential

DOI: 10.1021/acs.langmuir.9b00139
Langmuir 2019, 35, 7121−7128

by using Laser Doppler electrophoresis on a Zetasizer Nano (Malvern Instruments).

Fluorescence Microscopy for Qualitative Assessment of Surface Modification. To qualitatively assess the success of the modification of the gold-coated silicon slides, the adhesion of negatively charged fluorescently labeled nanoparticles at three pH values was imaged by using fluorescence microscopy. To this end, chemically modified gold-coated silicon slides were incubated with 1 μL/mL nanoparticle dispersions in 1 mM EDTA buffers with pH values of 2.0, 2.5, and 7.5. After 2 h, the slides were washed with 1 mM EDTA buffer having the same pH as the nanoparticle dispersion and dried by using a gentle air stream. The slides were imaged by using a Nikon Eclipse E600 with a GFP filter set in conjunction with a Photometrics Coolsnap Pro CF monochrome camera and Media Cybernetics imaging software.

Atomic Force Microscopy. Atomic force microscopy (AFM) was performed on nonmodified and chemically modified gold-coated silicon slides that were incubated for 4 h with 1 μL of nanoparticle dispersion per mL of 1 mM EDTA buffer at pH values of 2.5, 5, and 7 using a NanoWizard 3 NanoOptics AFM System (JPK Instruments) in QI (Quantitative Imaging) mode. The NanoWizard 3 FM was equipped with an OLTESPA (70 kHz, 2 N/m) microcantilever. The following settings were used: setpoint, 0.3 V; Z length, 100 nm; pixel time, 15.0 ms; fast axis, 2.0 μm; slow axis, 2.0 μm. The data was analyzed in Gwyddion software version 2.5.

Fluorescent Nanoparticle Adhesion Assay. To investigate the applicability of the FNAA to determine the pK_a of functionalized gold surfaces, the surface pK_a of the chemically modified gold-coated silicon slides was determined by using the general principles of the FNAA.[9] This assay is based on electrostatic interactions between electrochemically charged surfaces and oppositely charged nanoparticles as a function of the pH. Because only one side of the gold-coated silicon slides was modified with pH-sensitive groups, the FNAA was adapted to determine the surface pK_a of the chemically modified gold-coated side (i.e., for each pH determination, nanoparticle adhesion was determined for gold-coated silicon slides and silicon control slides).

For each titration, 1 μL/mL nanoparticle dispersions in 1 mM EDTA with pH values from 10.5 to 2 (in steps of ~0.5 pH values per dispersion) were prepared by using 0.1 or 0.01 M HCl to adjust the pH. At each pH value, 750 μL of the nanoparticle dispersion was transferred to a 1.5 mL cuvette in triplicate. Next, to each of these cuvettes, (1) a gold-coated silicon slide, (2) a silicon control slide, or (3) no silicon slide (control) was added, which was subsequently sealed with Parafilm and covered in aluminum foil to protect the fluorescent nanoparticles from light. For each chemically modified gold-coated silicon slide, titration was performed at least twice. After 4 h of shaking at 500 rpm (IKA VXR Basic Vibrax orbital shaker), from each sample, two aliquots of 200 μL were transferred to a flat-bottom black 96-wells plate. Fluorescence was measured on a Tecan Infinite M1000 plate reader at an excitation wavelength of 520 nm and an emission wavelength of 540 nm.

Surface-Specific Nanoparticle Binding. To determine the surface-specific binding of nanoparticles onto chemically modified gold surfaces, first, the pH-dependent binding percentage of nanoparticles per cm^2 onto the silicon control slides (B_{Si}) was calculated according to eq 1

$$B_{Si} = (1 - [Fluo_{Si}/Fluo_{Contr}])/2 \times 100\% \quad (1)$$

where $Fluo_{Si}$ is the fluorescence of the nanoparticle dispersion that was incubated with a silicon control slide, and $Fluo_{Contr}$ is the fluorescence of the nanoparticle dispersion that was not incubated with a silicon slide, which served as a control for nonspecific adhesion of nanoparticles to the cuvette.

Next, the total binding of nanoparticles onto the gold-coated silicon slides (B_{Au}) as a function of the pH was calculated according to eq 2

$$B_{Au} = (1 - [Fluo_{Au}/Fluo_{Contr}]) \times 100\% \quad (2)$$

where $Fluo_{Au}$ is the fluorescence of the nanoparticle dispersion that was incubated with a gold-coated silicon slide. Binding data was smoothed by averaging the binding percentage at five successive pH values.

Because the gold-coated silicon slides expose the 1 cm^2 silicon surface (noncoated side), the percentage of specific binding of nanoparticles onto the chemically modified gold side ($B_{Au\text{-}specific}$) was calculated by subtracting the percentage of the nanoparticles that bound onto the 1 cm^2 silicon surface (B_{Si}) from B_{Au} (see eq 3)

$$B_{Au-specific} = B_{Au} - B_{Si} \quad (3)$$

Calculation of Surface pK_a. To compare the binding of nanoparticles onto the different functionalized gold surfaces, first, the minimum (B_{Min}) and maximum (B_{Max}) percentages of nanoparticle binding onto each chemically modified gold-coated surface were calculated (horizontal bottom and top asymptotes, respectively) according to eq 4

$$B_{Au-specific} = B_{Min} + ([B_{Max} - B_{Min}]/[1 + 10^{(pKa-pH)}]) \quad (4)$$

Next, for each functionalized gold surface, at each pH value, nanoparticle binding was normalized between the minimum and maximum binding according to eq 5

$$\text{norm. surface charge} = ([B_{Au-specific} - B_{Min}]/[B_{Max} - B_{Min}]) \times 100\% \quad (5)$$

Finally, the normalized surface charge was plotted as a function of the pH, and an S-shaped curve with its 95% confidence interval was calculated according to the Henderson–Hasselbalch equation. The pK_a was defined and calculated as the midpoint of the S-shaped curve. All calculations were performed by using GraphPad Prism 7.

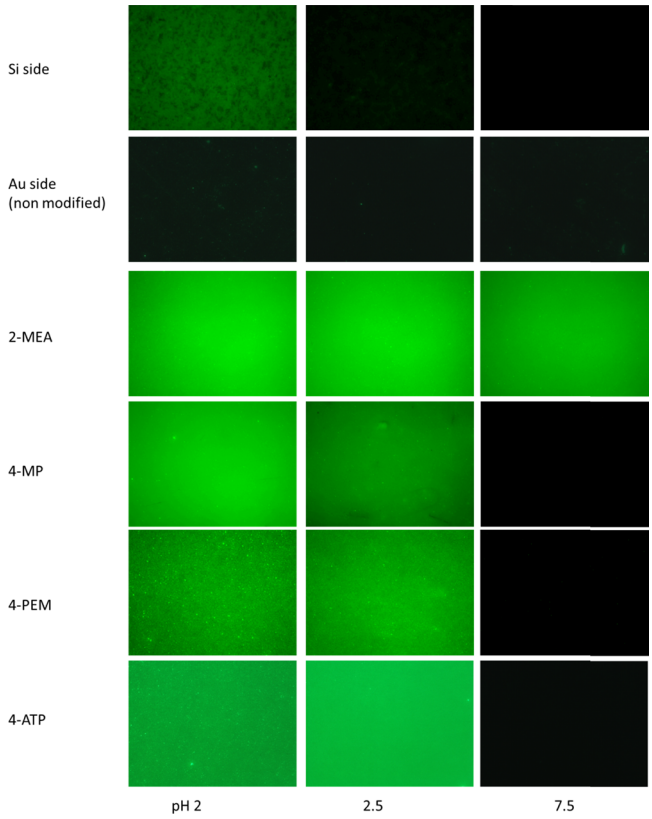

Figure 2. Representative fluorescence microscopy images (200-fold magnification) of silicon and chemically modified gold-coated silicon surfaces that had been incubated with negatively charged fluorescently labeled nanoparticles at different pH values. Abbreviations: 2-MEA, 2-mercaptoethylamine; 4-MP, 4-mercaptopyridine; 4-PEM, 4-pyridylethylmercaptan; 4-ATP, 4-aminothiophenol.

DOI: 10.1021/acs.langmuir.9b00139
Langmuir 2019, 35, 7121–7128

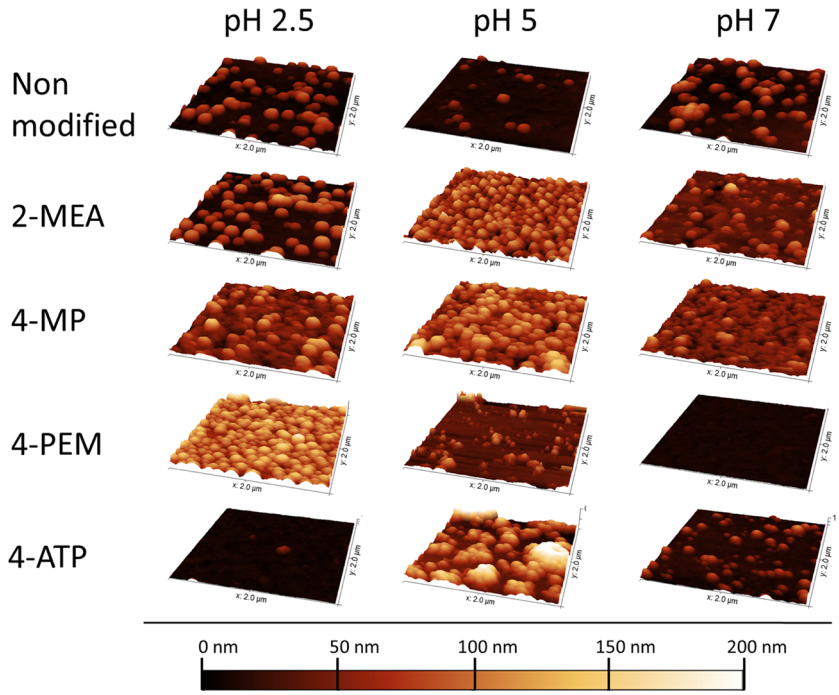

Figure 3. AFM images of chemically modified gold-coated silicon surfaces that had been incubated with negatively charged nanoparticles at different pH values. The dimensions of the images are 2000 × 2000 × 200 nm ($l \times w \times h$), and the color scale bar indicates the thickness of the surface coating. Abbreviations: 2-MEA, 2-mercaptoethylamine; 4-MP, 4-mercaptopyridine; 4-PEM, 4-pyridylethylmercaptan; 4-ATP, 4-aminothiophenol.

RESULTS

pH-Dependent Stability of Nanoparticles. To determine the pK_a of gold surfaces that have been modified with basic molecules by using oppositely charged (sulfate-modified) nanoparticles, the nanoparticles should be physicochemically stable in the investigated pH range. The hydrodynamic diameter (94 ± 1 nm), PDI (0.16 ± 0.01), and ζ-potential (−58 ± 6 mV) of the negatively charged nanoparticles did not noticeably change in the investigated pH range (pH 2−10). Furthermore, the fluorescence intensity of the nanoparticles was independent of the pH within the tested range between 3 and 12 (results not shown). So, these nanoparticles are suitable to be used to analyze gold surfaces that have been modified with basic groups having surface pK_a values ranging from 3 to 9.

Assessment of Surface Modification. The success of the chemical modification of the gold surfaces was assessed by imaging the adhesion of the negatively charged fluorescently labeled nanoparticles at three different pH values onto the gold-coated silicon slides using fluorescence microscopy. As shown in Figure 2, the nanoparticles bound onto plain (uncoated) silicon surfaces at a pH value of 2 but hardly bound at pH values of 2.5 and 7.5. Furthermore, hardly any fluorescence was detected on the nonmodified gold surfaces. In contrast, the fluorescently labeled negatively charged fluorescent nanoparticles bound onto the chemically modified gold surfaces in a pH-dependent manner. Therefore, this data qualitatively shows that the modification of the gold surfaces with the four basic molecules was successful.

Besides fluorescence imaging, the chemically modified gold surfaces were imaged by AFM (see Figure 3). AFM imaging revealed that the nanoparticle adsorption is substantially higher at low pH (pH 2.5 and 5) than at pH 7. Furthermore, it was observed that some nanoparticle adhesion occurred onto nonmodified gold surfaces (which was also observed by fluorescence imaging). In general, more nanoparticles were counted onto the modified gold surfaces as compared to the nonmodified surfaces. However, AFM is much more time-consuming and analyzes a much smaller area (1 μm^2) than fluorescence imaging (0.2 mm^2).

pK_a Determination of Chemically Modified Gold Surfaces. After it was shown that the gold surfaces were successfully modified with a panel of basic groups, the FNAA (see Materials and Methods) was performed. As shown in Figure 4 (left side), the binding of negatively charged nanoparticles onto the chemically modified gold-coated silicon slides and silicon control slides was determined as a function of the pH. Because the fluorescently labeled negatively charged nanoparticles also bound onto uncoated silicon surfaces at low pH values, the binding of these nanoparticles onto the gold-coated silicon slides was corrected for nanoparticle adhesion onto the silicon side according to eq 3. As shown in Figure 4 (right side), the maximum binding of negatively charged nanoparticles onto gold surfaces (pH ∼2.5) modified with 2-MEA, 4-MP, or 4-PEM was comparable (21 ± 4, 26 ± 14, and 25 ± 3%, respectively) but higher for 4-ATP-coated gold surfaces (41 ± 15%).

To calculate the pK_a value of gold surfaces that were modified with basic groups, the pH-dependent binding of the negatively charged fluorescently labeled nanoparticles onto the gold-coated silicon slides was normalized to the minimum and maximum binding (normalized surface charge) according to eq 5. As shown in Figure 5, the normalized surface charge of the gold-coated silicon surfaces modified with the four different gold-specific modifiers was significantly distinguishable from each other (as the 95% confidence intervals did not overlap between normalized surface charges of 10 and 90%). The calculated pK_a values were 7.4 ± 0.3 (2-MEA), 3.7 ± 0.1 (4-MP), 5.0 ± 0.1 (4-PEM), and 5.4 ± 0.1 (4-ATP). This data shows that the FNAA is a powerful tool for distinguishing between pH-sensitive surface groups having different pK_a values on gold surfaces that are modified with basic molecules.

DOI: 10.1021/acs.langmuir.9b00139
Langmuir 2019, 35, 7121−7128

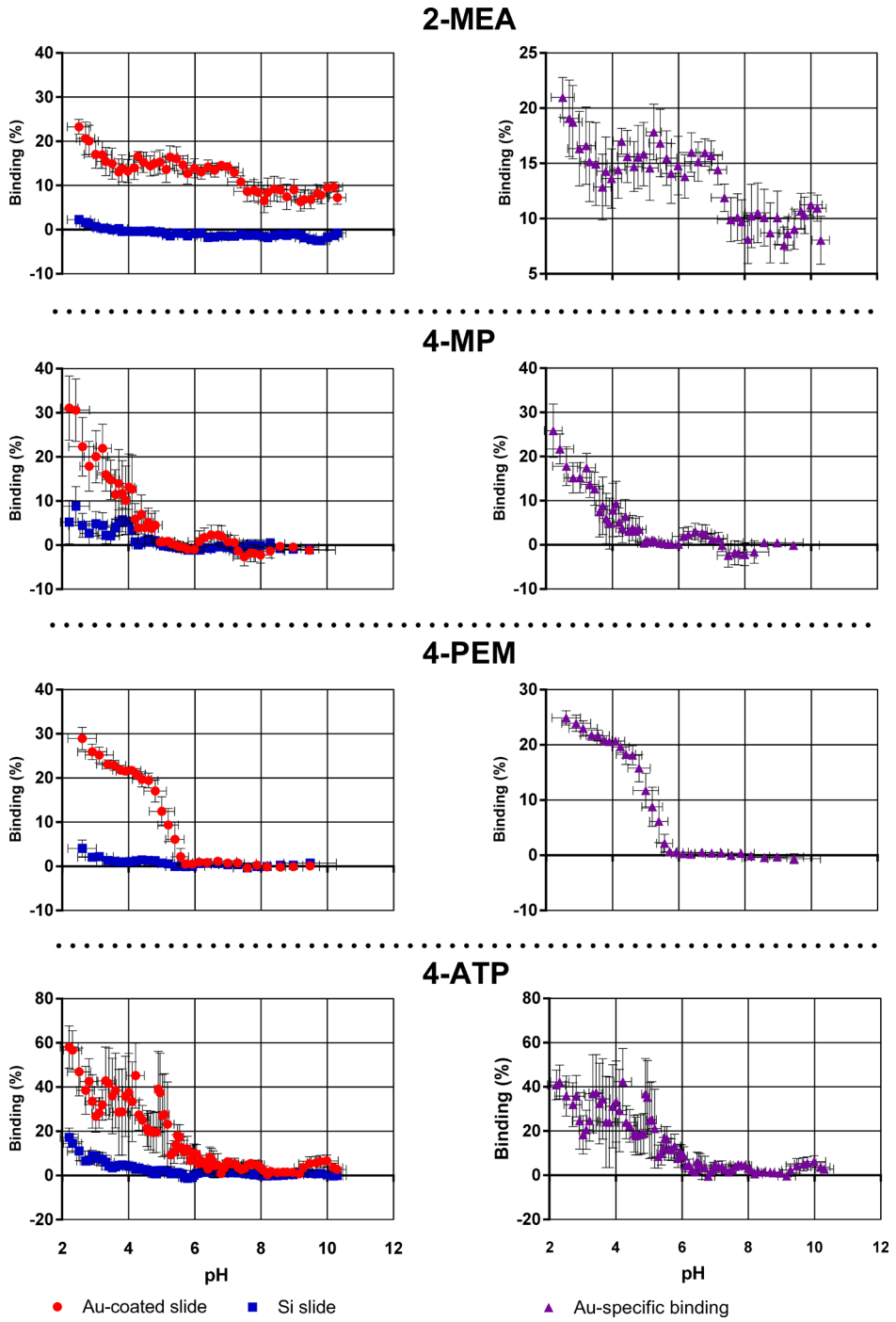

Figure 4. Results of FNAA of negatively charged fluorescently labeled nanoparticles onto silicon slides (B_{Si}) and gold-coated silicon slides modified with pH-sensitive groups (B_{au}) (left) and gold-coated silicon slides corrected for nanoparticle adhesion onto the silicon side ($B_{Au\text{-}specific}$) (right). Abbreviations: 2-MEA, 2-mercaptoethylamine; 4-MP, 4-mercaptopyridine; 4-PEM, 4-pyridylethylmercaptan; 4-ATP, 4-aminothiophenol. Values are represented as mean ± SEM.

DISCUSSION

Well-characterized functionalized gold surfaces have great potential for pharmaceutical, biological, and biomedical applications, such as DNA delivery,[6] pH-dependent drug delivery to cancer cells,[13] and biosensors.[3] In this work, gold surfaces were successfully modified with a panel of different basic molecules, which was confirmed by using negatively charged fluorescently labeled nanoparticles and fluorescence microscopy. Such a method using nanoparticles and fluorescence microscopy is a fast, easy, and cheap approach to check whether the surface modification is successful.

The modification of gold-coated silicon slides with 4-MP, 4-PEM, and 4-ATP resulted in pH-sensitive surfaces that are highly positively charged in a (slightly) acidic environment and that are (almost) uncharged at physiological pH (7.4). Therefore, these surface modifiers have potential for, for example, pH-dependent drug delivery whereby anionic drugs may be adhered to the gold surface at a (slightly) acidic pH (positively charged surface) and can be released at physiological pH (noncharged surface).[10,14] However, the binding of negatively charged nanoparticles onto 2-MEA-modified gold surfaces

DOI: 10.1021/acs.langmuir.9b00139
Langmuir 2019, 35, 7121−7128

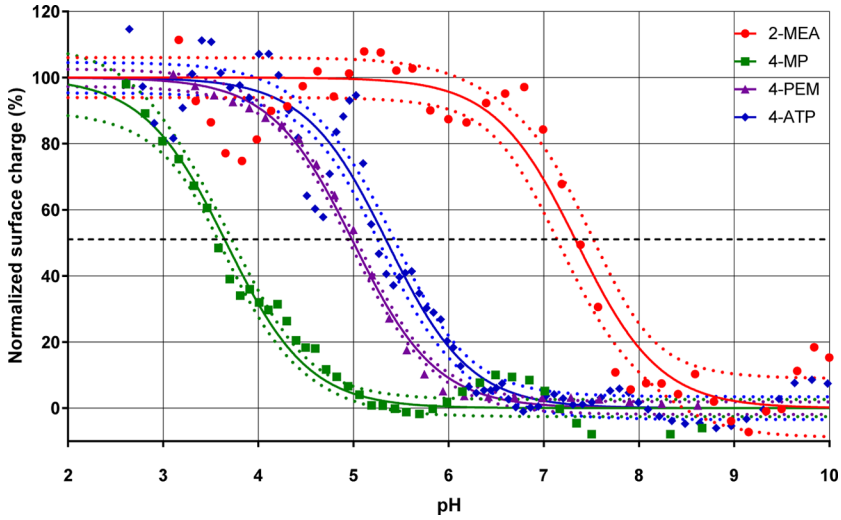

Figure 5. Normalized surface charge of chemically modified gold-coated silicon surfaces as a function of the pH, as determined by FNAA. The black dashed line indicates the surface pK_a where the normalized surface charge is 50% of its maximal value. Abbreviations: 2-MEA, 2-mercaptoethylamine; 4-MP, 4-mercaptopyridine; 4-PEM, 4-pyridylethylmercaptan; 4-ATP, 4-aminothiophenol. Values are represented as mean ± 95% confidence intervals (dotted lines).

decreased from 20 to 10% but did not reach 0%, indicating that 2-MEA surfaces have two surface pK_a values, one of which is above 10 (2-MEA in solution has a pK_a of 10). Similarly to 2-MEA on gold (ethylamine surface groups), APTES-modified silicon (propylamine surface groups) resulted in surfaces having two pK_a values, one of 7 and the second of 10.[9] However, the potential second surface pK_a was not further investigated because the binding of negatively charged nanoparticles at higher pH values is not relevant under physiological conditions and therefore was outside the scope of this research.

To determine the pK_a of functionalized surfaces, a variety of methods have been developed, such as an indirect laser-induced temperature jump method,[15] interfacial impedance,[16,17] differential capacitance measurements,[18] reductive desorption,[19] electrochemical titration,[20,21] piezoelectric quartz crystal microbalance,[22] surface potential measurements,[23,24] optical absorption spectroscopy,[25] surface enhanced Raman scattering,[26−29] chemical force microscopy,[30] faradaic impedance titration,[31] and contact angle titration.[29] However, most of these methods require expensive equipment, are complicated, or lack accuracy because of their invasive character.[9,32] As fluorescence spectroscopy is widely available in pharmaceutical and biological laboratories, an FNAA may be a good alternative to the methods described above. However, an FNAA, as previously reported,[9] is not directly applicable to determine the surface pK_a of gold-coated silicon surfaces that have been modified with basic molecules, which was therefore adapted in this study.

In this research, it was shown that negatively charged fluorescently labeled nanoparticles bound onto plain silicon surfaces at low pH values. This was expected because the isoelectric point of silicon surfaces containing silanol groups is between 0.5 and 3.5.[33] Below the isoelectric point, the surface is positively charged and capable of binding negatively charged nanoparticles. Therefore, the adhesion of nanoparticles onto gold-coated silicon slides was corrected for the adhesion of nanoparticles onto the silicon side.

The surface pK_a values obtained by using an FNAA were compared to those reported in the literature (shown in Table 1). This shows that different surface pK_a values have been found for the same chemically modified gold surfaces when using different methods (e.g., Fourier-transform surface-enhanced Raman scattering, chemical force microscopy, and faradaic impedance titration[12,18,19,26,28−31]). Therefore, these literature values illustrate that the determination of surface pK_a values is not straightforward and the outcome may be dependent on the method used (several methods have different measurement principles). The surface pK_a values obtained by using the FNAA (at least for 2-MEA and 4-MP) are in the same range as the values reported in the literature. To our knowledge, in the literature, there is only one report where two of the same gold-reactive molecules have been used as in this study. In the study

Table 1. Surface pK_a (with 95% Confidence Interval (CI)) of Chemically Modified Gold Surfaces Obtained by Our Fluorescent Nanoparticle Adhesion Assay (FNAA) or via Various Methods Reported in the Literature[a]

gold-reactive molecule	pK_a FNAA (mean, 95% CI)	pK_a from the literature	method used in the literature	reference
2-MEA	7.4 (7.1−7.6)	3.4−5	Fourier-transform (FT) surface-enhanced Raman scattering (FT-SERS)	26
		5	FT-SERS	27
		6.4−6.8	reductive desorption	19
		7	chemical force microscopy	30
		8.6	faradaic impendence titration	31
4-MP	3.7 (3.5−3.8)	3.9	SERS	29
		∼4	contact angle titration	29
		4.6	differential interfacial capacitance	18
		5.3	SERS with Gouy−Chapmann model	29
		7.5	cyclic voltammetry	12
4-PEM	5.0 (4.9−5.1)	3.3	FT-SERS (note that authors refer to an unpublished work and published the same work in two journals...)	28
4-ATP	5.4 (5.2−5.5)	6.9	differential interfacial capacitance	18

[a]Abbreviations: 2-MEA, 2-mercaptoethylamine; 4-MP, 4-mercaptopyridine; 4-PEM, 4-pyridylethylmercaptan; 4-ATP, 4-aminothiophenol.

DOI: 10.1021/acs.langmuir.9b00139
Langmuir 2019, 35, 7121−7128

by Bryant and Crooks, the surface pK_a values of gold surfaces modified with 4-MP and 4-ATP were determined by using differential interfacial capacitance.[18] Although the surface pK_a values obtained in our study using the FNAA were about 1 pK_a unit lower, the relative difference between the two chemically modified gold surfaces was similar to the difference found by them (~2 pK_a-unit difference). Therefore, these results show that the FNAA is a powerful tool for studying nanoparticle−surface interaction and is a fairly easy and cheap alternative to conventional methods to determine the surface pK_a of chemically modified gold surfaces.

CONCLUSIONS

In this work, we have successfully modified gold surfaces with a panel of basic groups with different pK_a values that are potentially useful for pharmaceutical applications. We have shown that the success of the modification of gold surfaces with basic molecules can be assessed easily and fast by using negatively charged fluorescently labeled nanoparticles and fluorescence microscopy. Finally, by determining the pH-dependent nanoparticle adhesion onto gold-coated silicon slides corrected for nanoparticle adhesion onto the silicon side, the pK_a of gold surfaces modified with a variety of basic molecules can be determined.

AUTHOR INFORMATION

Corresponding Author

*E-mail: maadenkvander@lacdr.leidenuniv.nl.

ORCID

K. van der Maaden: 0000-0003-0682-2403

Author Contributions

‡K.v.d.M. and P.S. contributed equally to this work.

Notes

The authors declare no competing financial interest.

ACKNOWLEDGMENTS

We thank N. Benne and M. Glandrup of the division of BioTherapeutics of Leiden University for their help with the AFM measurements.

REFERENCES

(1) Shukla, R.; Bansal, V.; Chaudhary, M.; Basu, A.; Bhonde, R. R.; Sastry, M. Biocompatibility of gold nanoparticles and their endocytotic fate inside the cellular compartment: a microscopic overview. *Langmuir* **2005**, *21*, 10644−54.

(2) van der Maaden, K.; Jiskoot, W.; Bouwstra, J. Microneedle technologies for (trans)dermal drug and vaccine delivery. *J. Controlled Release* **2012**, *161*, 645−55.

(3) Ranamukhaarachchi, S. A.; Padeste, C.; Dübner, M.; Häfeli, U. O.; Stoeber, B.; Cadarso, V. J. Integrated hollow microneedle-optofluidic biosensor for therapeutic drug monitoring in sub-nanoliter volumes. *Sci. Rep.* **2016**, *6*, 29075.

(4) Prow, T. W.; Chen, X.; Prow, N. A.; Fernando, G. J. P.; Tan, C. S. E.; Raphael, A. P.; Chang, D.; Ruutu, M. P.; Jenkins, D. W. K.; Pyke, A.; Crichton, M. L.; Raphaelli, K.; Goh, L. Y. H.; Frazer, I. H.; Roberts, M. S.; Gardner, J.; Khromykh, A. A.; Suhrbier, A.; Hall, R. A.; Kendall, M. A. F. Nanopatch-targeted skin vaccination against West Nile Virus and Chikungunya virus in mice. *Small* **2010**, *6*, 1776−84.

(5) Fernando, G. J. P.; Chen, X.; Prow, T. W.; Crichton, M. L.; Fairmaid, E. J.; Roberts, M. S.; Frazer, I. H.; Brown, L. E.; Kendall, M. A. F. Potent immunity to low doses of influenza vaccine by probabilistic guided micro-targeted skin delivery in a mouse model. *PLoS One* **2010**, *5*, No. e10266.

(6) Ding, Y.; Jiang, Z.; Saha, K.; Kim, C. S.; Kim, S. T.; Landis, R. F.; Rotello, V. M. Gold nanoparticles for nucleic acid delivery. *Mol. Ther.* **2014**, *22*, 1075−1083.

(7) Dreaden, E. C.; Austin, L. A.; Mackey, M. A.; El-Sayed, M. A. Size matters: gold nanoparticles in targeted cancer drug delivery. *Ther. Delivery* **2012**, *3*, 457−78.

(8) Spyratou, E.; Makropoulou, M.; Efstathopoulos, E.; Georgakilas, A.; Sihver, L. Recent Advances in Cancer Therapy Based on Dual Mode Gold Nanoparticles. *Cancers (Basel)* **2017**, *9*, 173.

(9) van der Maaden, K.; Sliedregt, K.; Kros, A.; Jiskoot, W.; Bouwstra, J. Fluorescent nanoparticle adhesion assay: a novel method for surface pKa determination of self-assembled monolayers on silicon surfaces. *Langmuir* **2012**, *28*, 3403−11.

(10) van der Maaden, K.; Yu, H.; Sliedregt, K.; Zwier, R.; Leboux, R.; Oguri, M.; Kros, A.; Jiskoot, W.; Bouwstra, J. A. Nanolayered chemical modification of silicon surfaces with ionizable surface groups for pH-triggered protein adsorption and release: application to microneedles. *J. Mater. Chem. B* **2013**, *1*, 4466−4477.

(11) van der Maaden, K.; Tomar, J.; Jiskoot, W.; Bouwstra, J. Chemical modifications of silicon surfaces for the generation of a tunable surface isoelectric point. *Langmuir* **2014**, *30*, 1812−9.

(12) de F. Paulo, T.; Abruña, H. D.; Diógenes, I. C. N. Thermodynamic, kinetic, surface pKa, and structural aspects of self-assembled monolayers of thio compounds on gold. *Langmuir* **2012**, *28*, 17825−31.

(13) Madhusudhan, A.; Reddy, G.; Venkatesham, M.; Veerabhadram, G.; Kumar, D.; Natarajan, S.; Yang, M.-Y.; Hu, A.; Singh, S. Efficient pH dependent drug delivery to target cancer cells by gold nanoparticles capped with carboxymethyl chitosan. *Int. J. Mol. Sci.* **2014**, *15*, 8216−34.

(14) van der Maaden, K.; Varypataki, E. M.; Romeijn, S.; Ossendorp, F.; Jiskoot, W.; Bouwstra, J. Ovalbumin-coated pH-sensitive microneedle arrays effectively induce ovalbumin-specific antibody and T-cell responses in mice. *Eur. J. Pharm. Biopharm.* **2014**, *88*, 310−5.

(15) Smalley, J. F.; Geng, L.; Chen, A.; Feldberg, S. W.; Lewis, N. S.; Cali, G. An indirect laser-induced temperature jump study of the influence of redox couple adsorption on heterogeneous electron transfer kinetics. *J. Electroanal. Chem.* **2003**, *549*, 13−24.

(16) Opa Ilo, M.; Dojlido, J. Dissociation Equilibrium of O-Phthalic Acid on the Mercury Electrode. *J. Electroanal. Chem.* **1981**, *127*, 211−217.

(17) Dojlido, J.; Dmowska-stańczak, M.; Galus, Z. Adsorption and Dissociation Equilibrium of Benzoic Acid on the Mercury Electrode. *J. Electroanal. Chem.* **1978**, *94*, 107−122.

(18) Bryant, M. A.; Crooks, R. M. Determination of Surface pKa Values of Surface-Confined Molecules Derivatized with pH-Sensitive Pendant Groups. *Langmuir* **1993**, *9*, 385−387.

(19) Munakata, H.; Oyamatsu, D.; Kuwabata, S. Effects of ω-functional groups on pH-dependent reductive desorption of alkanethiol self-assembled monolayers. *Langmuir* **2004**, *20*, 10123−10128.

(20) Zhao, J.; Luo, L.; Yang, X.; Wang, E.; Dong, S. Determination of surface pK_a of SAM using an electrochemical titration method. *Electroanalysis* **1999**, *11*, 1108−1113.

(21) Dai, Z.; Ju, H. Effect of chain length on the surface properties of ω-carboxy alkanethiol self-assembled monolayers. *Phys. Chem. Chem. Phys.* **2001**, *3*, 3769−3773.

(22) Sugihara, K.; Shimazu, K.; Uosaki, K. Electrode potential effect on the surface pK_a of a self-assembled 15-mercaptohexadecanoic acid monolayer on a gold/quartz crystal microbalance electrode. *Langmuir* **2000**, *16*, 7101−7105.

(23) Betts, J. J.; Pethica, B. A. The Ionization Characteristics of Monolayers of Weak Acids and Bases. *Trans. Faraday Soc.* **1956**, *52*, 1581−1589.

(24) Caspers, J.; Goormaghtigh, E.; Ferreira, J.; Brasseur, R.; Vandenbranden, M.; Ruysschaert, J.-M. Acido-Basic Properties of Lipophilic Substances - a Surface-Potential Approach. *J. Colloid Interface Sci.* **1983**, *91*, 546−551.

DOI: 10.1021/acs.langmuir.9b00139
Langmuir 2019, 35, 7121−7128

(25) Mayya, K. S.; Patil, V.; Sastry, M. On the stability of carboxylic acid derivatized gold colloidal particles: The role of colloidal solution pH studied by optical absorption spectroscopy. *Langmuir* **1997**, *13*, 3944−3947.
(26) Cao, X. W. Study of electrode potential effect on acid-base behavior of ω-functionalized self-assembled monolayers using Fourier transform surface-enhanced Raman scattering spectroscopy. *J. Raman Spectrosc.* **2005**, *36*, 250−256.
(27) Nishiyama, K.; Kubo, A.; Ueda, A.; Taniguchi, I. Surface pK_a of amine-terminated self-assembled monolayers evaluated by direct observation of counter anion by FT-surface enhanced Raman spectroscopy. *Chem. Lett.* **2002**, 80−81.
(28) Nishiyama, K.; Tsuchiyama, M.; Kubo, A.; Seriu, H.; Miyazaki, S.; Yoshimoto, S.; Taniguchi, I. Conformational change in 4-pyridineethanethiolate self-assembled monolayers on Au(111) driven by protonation/deprotonation in electrolyte solutions. *Phys. Chem. Chem. Phys.* **2008**, *10*, 6935−6939.
(29) Yu, H.-Z.; Xia, N.; Liu, Z.-F. SERS titration of 4-mercaptopyridine self-assembled monolayers at aqueous buffer/gold interfaces. *Anal. Chem.* **1999**, *71*, 1354−1358.
(30) van der Vegte, E. W.; Hadziioannou, G. Acid-base properties and the chemical imaging of surface-bound functional groups studied with scanning force microscopy. *J. Phys. Chem. B* **1997**, *101*, 9563−9569.
(31) Molinero, V.; Calvo, E. J. Electrostatic interactions at self assembled molecular films of charged thiols on gold. *J. Electroanal. Chem.* **1998**, *445*, 17−25.
(32) He, H. X.; Li, C. Z.; Song, J. Q.; Mu, T.; Wang, L.; Zhang, H. L.; Liu, Z. F. Force titration of a carboxylic acid terminated self-assembled monolayer using chemical force microscopy. *Mol. Cryst. Liq. Cryst. Sci. Technol., Sect. A* **1997**, *294*, 99−102.
(33) Liu, X.; Cheng, J.; Lu, X.; Wang, R. Surface acidity of quartz: understanding the crystallographic control. *Phys. Chem. Chem. Phys.* **2014**, *16*, 26909−26916.

DOI: 10.1021/acs.langmuir.9b00139
Langmuir 2019, 35, 7121−7128